

# Sedimentation of Monodisperse and Bidisperse Hard-Sphere Colloidal Suspensions

M. A. Al-Naafa and M. Sami Selim

Dept. of Chemical Engineering and Petroleum Refining, Colorado School of Mines, Golden, CO 80401

*The effect of concentration on the sedimentation rate of uncharged rigid spheres was investigated. Three submicron sizes of silica spheres were prepared according to the method of Stöber (1968). The particles were sterically stabilized by chemisorption of stearyl alcohol at their surface by the method developed by van Helden (1981). The sterically stabilized silica particles dispersed in cyclohexane are known to behave as hard spheres. Monodisperse gravity sedimentation experiments were carried out for the various particle species over a wide concentration range of  $\phi = 0.003$  to  $\phi = 0.37$ , where  $\phi$  is the particle volume fraction in cyclohexane. The data for dilute suspensions ( $\phi < 0.03$ ) were found to be well described by Batchelor's equation:  $U/U_0 = 1 - 6.55\phi$ , where  $U$  is the sedimentation velocity and  $U_0$  is the Stokes velocity of a sphere in isolation. The data over the entire concentration range ( $0 < \phi < 0.37$ ) were found to be well described by the equation:  $U/U_0 = (1 - \phi)^{6.55}$ .*

*Bidisperse sedimentation experiments were also carried out, and the dilute data were found to be well represented by Batchelor's 1982 theory for polydisperse suspensions. The high concentration data were analyzed in terms of a model that does not distinguish between interactions of like and unlike particles.*

## Introduction

The sedimentation of a suspension of particles under the action of gravity has been studied extensively because of its importance in practical applications. The problem that has received the greatest attention is the sedimentation of a system of monodisperse spheres at very small particle Reynolds number. Theoretical studies concerned with this problem have been recently reviewed by Davis and Acrivos (1985). Only a few of the most relevant studies will be reviewed here. For a dilute random suspension of monodisperse spheres, Batchelor (1972) derived the following expression for the mean fall velocity  $U$  of a particle in the suspension:

$$\frac{U}{U_0} = 1 - 6.55\phi, \quad (1)$$

correct to order  $\phi$ . The  $O(\phi)$  correction includes only pairwise interactions. For sedimentation at moderate to high concentrations, Reed and Anderson (1980) developed an approximate

pairwise additive theory which reduces the intractable N-body hydrodynamic problem in a multiparticle suspension to appropriate combinations of two-body hydrodynamic interactions. For a monodisperse suspension of rigid particles which interact only through a hard sphere potential, their analysis yields

$$\frac{U}{U_0} = \frac{1 - 1.83\phi}{1 + 4.70\phi} \quad (2)$$

In arriving at this result, the concentration dependence of the pair distribution function was neglected, and instead, the dilute form was used. Consequently, the result overestimates the hindrance effect; giving negative values for the average sedimentation velocity at  $\phi > 0.546$ .

Glendinning and Russel (1982), applying a method developed by O'Brien (1979), derived a general expression for the sedimentation velocity of a random suspension of spheres which is valid for all volume fractions and arbitrary interaction potentials. In this expression, a hard sphere description of the suspension microstructure was used; particle interactions were,

Correspondence concerning this article should be addressed to M. S. Selim.

**Table 1. Sources of Published Experimental Results on Sedimentation of Uncharged Colloidal Suspensions**

Author/s (year)	Suspended Particles			Suspending Med.		$\phi$	$O(\phi)$ Coefficient	$n$
	Material	$a$ ( $\mu\text{m}$ )	$\rho_s$ ( $\text{g}/\text{cm}^3$ )	Fluid	$\rho_f$ ( $\text{g}/\text{cm}^3$ )			
Cheng and Schachman (1955)	PSL	0.13	1.052	Water	1.00	0.0038–0.0751	5.1	4.8
Newman et al. (1974)	DNA	0.0316	1.799	SSD	1.006	0.0005–0.0932	$6.7 \pm 0.8$	—
Kitchen and Preston (1976)	BSA	0.13	1.362	Water	1.00	0.0048–0.0593	8.5	11.18
Lundh (1980)	Human Transferrin	0.0035	1.379	Water	1.00	0.0035–0.2852	7.61	9.8
Lundh (1980)	BSA	0.0034	1.362	Water	1.00	0.1623–0.5294	—	13.45
Kops-Werkhoven and Fijnaut (1981)	Coated Silica Spheres	0.0165	1.61	Cyclo-hexane	0.78	0.0118–0.0955	$6.0 \pm 1$	$7.14 \pm 1$
Kops-Werkhoven and Fijnaut (1982)	Coated Silica Spheres	0.06	1.77	Cyclo-hexane	0.78	0.0040–0.4463	$6.0 \pm 1$	$5.90 \pm 1$
Buscall et al. (1982)	PSL	1.55	1.052	Water	1.00	0.0072–0.4785	$5.4 \pm 0.1$	$5.32 \pm 0.1$
Tackie et al. (1983)	Silica Spheres	0.3	2.1	Water	1.00	0.0051–0.2600	4.44	3.91
Al-Naafa and Selim (1992)	Coated Silica Spheres	0.242	2.061	Cyclo-hexane	0.775	0.0301–0.3039	—	$6.21 \pm 0.3$
	Coated Silica Spheres	0.130	1.924	Cyclo-hexane	0.775	0.0048–0.3700	$6.5 \pm 0.3$	$6.39 \pm 0.4$
	Coated Silica Spheres	0.065	1.780	Cyclo-hexane	0.775	0.0041–0.3311	$6.51 \pm 0.4$	$6.41 \pm 0.2$

Values for the  $O(\phi)$  coefficient were obtained by fitting the dilute range data to  $f(\phi) = 1 - \beta\phi$ .  
Values for the index  $n$  were obtained from the Richardson-Zaki plot.

however, approximated in a strictly pairwise manner. With these approximations, numerical results for the average sedimentation velocity were shown to conform correctly to the dilute limit. For  $\phi > 0.27$ , however, the predicted sedimentation velocity becomes negative, limiting the validity of the explicit calculations for highly concentrated suspensions. This failure was attributed by Glendinning and Russel to the lack of multibody hydrodynamics in the approximation for particle interactions. To account for the multibody hydrodynamic interactions, Brady and Durlofsky (1988) used the Rotne-Prager approximation and derived an explicit expression for the sedimentation velocity which is valid from the dilute limit all the way up to close packing. For a hard-sphere system, their analysis yields the following expression:

$$\frac{U}{U_0} = 1 + \phi - \frac{1}{5}\phi^2 - \frac{6}{5}\phi \left( \frac{5 - \phi + \frac{1}{2}\phi^2}{1 + 2\phi} \right) \quad (3)$$

This expression gives a value of 5 for the first-order correction to the Stokes velocity which is to be contrasted with Batchelor's value of 6.55.

Quantitative evaluation of theories for either dilute or concentrated suspensions ultimately depends on comparison with experimental data. A number of observations of the settling speed of uniform colloidal spheres (such as polymer latexes and proteins) in a dilute liquid suspension have been made,

usually under conditions such that the double layer thickness is a small fraction of the sphere radius (corresponding to a fairly high electrolytic strength of the liquid). Data from these investigations are summarized in Table 1. As seen from the table, the observed values for the  $O(\phi)$  coefficient vary between 4 and 8. Experiments with an  $O(\phi)$  coefficient less than Batchelor's theoretical value of 6.55 were discussed by Batchelor and Wen (1982). These authors noted that the difference between the observed and theoretical value for the  $O(\phi)$  coefficient could be a consequence of van der Waals attractive forces between the particles leading to an excess number of close pairs whose common speed of fall exceeds the fall speed of an isolated sphere. On the other hand, experiments with the  $O(\phi)$  coefficient larger than 6.55 appear to have been confounded by residual effects of long-range Coulomb repulsion interparticle potentials causing the particles to repel one another and thus leading to a deficiency in close pairs. The sedimentation data of fd bacteriophage DNA by Newman et al. (1974) appear to be free of both problems. Their measured value of  $6.7 \pm 0.8$  for the  $O(\phi)$  coefficient agrees well with Batchelor's theoretical value.

It is worth noting, however, that comparison of theoretical results for the hindered settling function with experimental data for proteins is not completely quantitative since the proteins do not conform exactly to a hard sphere system despite the relatively high ionic strengths of the solvents used. Also, significant uncertainty enters through the conversion of protein mass concentrations to volume fractions which greatly magnifies small errors in the data. On the other hand, latex particles

as those used by Cheng and Schachman (1955) and Buscall et al. (1982) are better suited as a test substance since they are fairly spherical and can be prepared with a high degree of uniformity with respect to particle size. However, these particles exhibit a swelling behavior in nonpolar solvents. Silica spheres prepared by the Stöber process (Stöber et al., 1968), however, appear to be free from both problems. Tackie et al. (1983) measured the sedimentation rate of unchanged silica spheres of radius  $0.6\ \mu\text{m}$  in the concentration range  $0.005 < \phi < 0.26$ . The silica particles were dispersed in water and the pH was adjusted with HCl to about 3, which is close to the isoelectric point of silica. Their measurements gave a value of 4.44 for the first-order correction to the Stokes velocity. The deviation of this value from the theoretical value of 6.55 could be a consequence of van der Waals attractions which become significant near the i.e.p.

An alternate method for preparing uncharged silica spheres involves steric stabilization. In this method, the particles are sterically stabilized in a suitable solvent by solvated aliphatic chains adsorbed (or grafted) on the particle surface. In the simplest terms, the adsorbed layer can be regarded as providing a barrier around each particle, preventing their close approach to one another. Moreover, the grafted aliphatic chains in a solvent with refractive index equal to that of the particles, will screen van der Waals attractions between the particle cores, provided that the surface coverage is complete. This method was adopted by van Helden and Vrij (1980) for the preparation of uncharged silica spheres dispersed in cyclohexane. Short aliphatic chains (18 carbon atoms) were chemically adsorbed (grafted) on the surface of silica spheres prepared by the Stöber process. In this way, the particles are sterically stabilized and can be dispersed in a nonpolar solvent with a suitable index of refraction. Time-averaged light scattering experiments proved that these silica particles dispersed in cyclohexane behave as hard spheres. The osmotic compressibility was found to be fairly well described by the Carnahan-Starling equation for hard spheres in particular at high concentrations up to a volume fraction of 40%. This system then serves as a hard-sphere model colloid and may be used to test the correctness of the existing theories by experiments. This system was used by Kops-Werkhoven and Fijnaut (1981, 1982) for measurement of the sedimentation rate of hard-sphere colloidal suspensions. They reported a value of  $6.0 \pm 1$  for the  $O(\phi)$  coefficient. The lack of agreement between this value and the theoretical value of 6.55 was explained by Batchelor and Wen (1982) to be due to residual attractive van der Waals forces between the coated particles. Apparently, the van der Waals attractions between the particle cores were not completely screened due to incomplete coverage of the surface of the particles by the hydrocarbon chains.

**Table 2. Radius of Silica Particles in Alcosols as a Function of TEOS/Ammonium Hydroxide/Alcohol Ratios**

Particle Type	Volume Ratio			Radius $a_{EM}$ (nm)
	TEOS	NH <sub>4</sub> OH	Alcohol	
$S_1$	1	5.2	24*	$242 \pm 12$
$S_2$	1	2.05	23.23**	$130 \pm 7$
$S_3$	1	1.8	26.20**	$65 \pm 4.5$

\* N-Propanol

\*\* Ethanol

In the present study, we report sedimentation data over a wide concentration range for three different sizes of coated silica particles dispersed in cyclohexane. Complete coverage of the particle surface by the hydrocarbon chains was monitored by measuring the carbon content of the spheres. In addition, sedimentation data for bidisperse suspensions over a wide concentration range are obtained. The data collected are compared with predictions from available theories.

## Particle Preparation

Silica particles dispersed in alcohol (here called alcosols) were prepared according to the method of Stöber et al. (1968). In this method, tetraethyl orthosilicate (TEOS) is hydrolyzed in a mixture of alcohol, ammonia, and water. Two types of reactions occur in the formation of silica particles: silanol groups are formed by hydrolysis and siloxane bridges are formed by a condensation polymerization reaction. Three different sizes ( $S_1$ ,  $S_2$ ,  $S_3$ ) were prepared. The volume ratios of TEOS/ammonium hydroxide/alcohol are given in Table 2. All chemicals used were of reagent grade supplied by Kodak and Aldrich.

Ammonium hydroxide and alcohol were mixed in a reaction vessel. TEOS was then added and the reaction mixture was stirred at  $25 \pm 0.1^\circ\text{C}$  for several hours depending on the particle size. After the allowed time of reaction, samples for electron microscope examination were taken. Transmission electron microscope measurements were performed with a Philips EM 400 apparatus. The electron microscopy pictures showed that the particles were spherically symmetric and of uniform size. It was found that the maximal sphericity and uniformity of the particles depended on the use of extremely pure reactants and extreme care in cleaning glassware that touches the reactants. Thus, all the TEOS and the alcohol were redistilled several times in specially constructed vacuum fractionators. Only the middle one-third cut was retained in each distillation. In this manner, it was possible to extract reactants with a purity of almost 100%. Further details of the preparation process are available (Al-Naafa, 1990).

The water in the aqueous silica sols from the Stöber process was next removed by distillation at  $78^\circ\text{C}$ . Substantial amounts of anhydrous ethanol was added gradually to the aqueous silica sol during the water distillation. The addition of alcohol was continued until the water content in the distillation pot was reduced to below 0.1%, thus producing an essentially anhydrous silica sol in the still. For the  $S_1$  particles, it was found that complete removal of the water from the silica sol was essential (Al-Naafa, 1990).

Next, the silica particles were sterically stabilized by chemisorption of stearyl alcohol at their surface by a method developed by Iler (1957) and subsequently used by van Helden and coworkers (1980, 1981). The hydrocarbon chains (18 carbon atoms) sticking out of the surface (see Figure 1) make the particles soluble in nonpolar solvents (for example, cyclohexane). The amount of stearyl alcohol used per each batch was 3 to 5 times the theoretical yield of silica. Esterification of the particles with stearyl alcohol was carried out under a nitrogen atmosphere at  $300^\circ\text{C}$  for the  $S_1$  particles and  $200$ – $250^\circ\text{C}$  for the  $S_2$  and  $S_3$  particles. In order to achieve complete coverage of the particle surface by aliphatic chains, a series of experiments were performed by changing the esterification time and monitoring the carbon content of the particles. The results

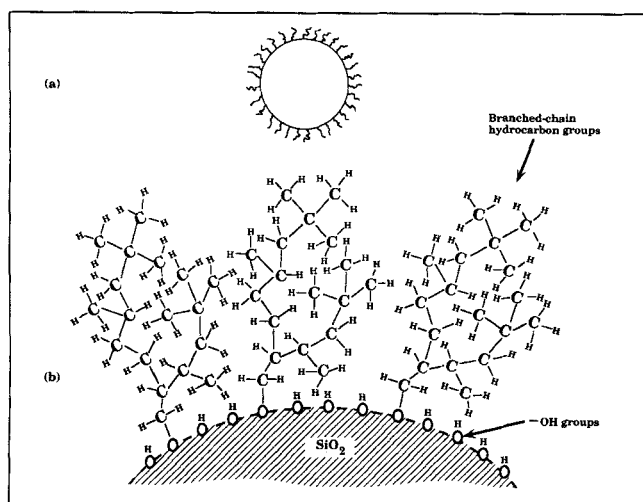


**Figure 1. (a) Schematic picture of a sterically stabilized silica particle. The nucleus consists of silicon dioxide ( $\text{SiO}_2$ ) and the surrounding layer consists of hydrocarbon chains (C-18). (b) Diagrammatic illustration of a portion of the surface of the modified particle in section.**

of these experiments are shown in Figure 2 for the  $S_1$  particles. As the figure indicates, the maximum carbon content was obtained when the esterification process lasted at least 10 hours. For the  $S_2$  and  $S_3$  particles, respectively, 8 and 5 hours for the esterification time were sufficient to ensure complete coverage of the particles by the hydrocarbon chains. Adsorption with methyl red as described by Ballard et al. (1961) was also carried out in order to further ensure maximum degree of esterification and zero hydroxylated surface area.

The separation of the coated silica particles from the large excess of stearyl alcohol was achieved by a combination of nitrogen flow distillation and centrifugation. After distillation, the particles were dispersed in cyclohexane and the hot suspension was ultracentrifuged to separate the coated particles from the excess octadecanol. The supernatant with remaining octadecanol was discarded. The silica particles were again re-dispersed in cyclohexane and the above procedure was repeated. Finally the coated particles were dried at  $80^\circ\text{C}$  for 24 hours under nitrogen atmosphere. Sample electron micrographs of the coated particles are shown in Figures 3a through 3c.

### Particle Characterization

Electron micrographs were taken to determine shape, size, and size distribution of the coated particles (Figure 3). Measurements were performed with a Philips EM 400 apparatus. Carrier grids covered with carbon-coated Parlodion films were dipped in a dilute dispersion and electron micrographs were taken of the particles retained on the film. From Figure 3, it can be seen that the particles are fairly spherical. The size and size distribution of the particles were measured from these pictures and are given in Table 3.

The partial specific volume of the coated particles in cyclohexane was determined from density measurements on silica particle suspensions with varying particle concentration. The

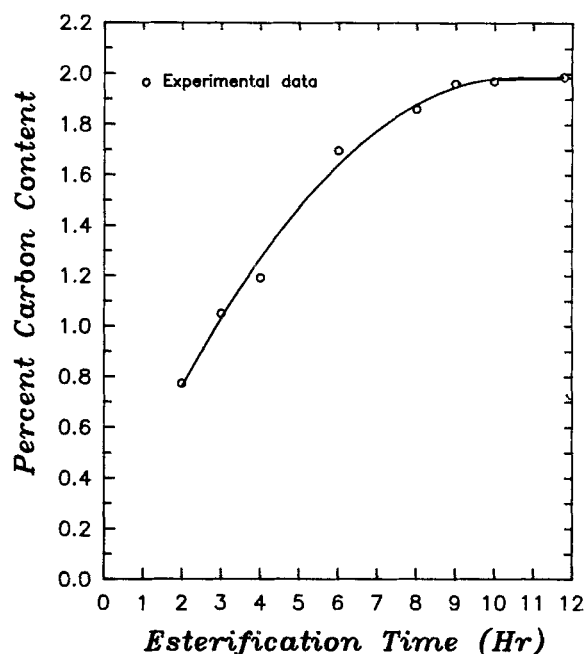


**Figure 2. Percent carbon content of the  $S_1$  particles vs. esterification time.**

suspensions were prepared by dispersing a known weight of the dry coated particles into a given weight of cyclohexane. The particles were dispersed by sonication in an ultrasonic water bath (type Bransonic 52) for approximately one hour. Density measurements of the suspensions were carried out using Weld pycnometers at  $25 \pm 0.1^\circ\text{C}$ . Figure 4 shows the reciprocal of the density of the suspension  $\rho^{-1}$  as function of the mass fraction of cyclohexane  $\omega_{cy}$ . From this figure the partial specific volume  $\bar{v}_i$  of the particles may be determined using the slope-intercept method (Prigogine and Defay, 1954). The intercept on the  $\rho^{-1}$  axis of a tangent to the curve at a particular composition yields  $\bar{v}_i$  at that composition. We may note from Figure 4 that the  $\rho^{-1}$  vs.  $\omega_{cy}$  curve, for each particle species, is essentially linear for  $0 < \omega_p < 0.5$ ;  $\omega_p$  being the mass fraction of the particles. Thus, the partial specific volumes of the particles are essentially independent of composition in this concentration range. The obtained values for the partial specific volumes of the three particle species are listed in Table 3.

The hydrodynamic specific volume  $\bar{v}_h$  of the particles was determined from viscosity measurements according to the method suggested by Mewis et al. (1989). The hydrodynamic specific volume relates the particle volume fraction  $\phi$  to the mass concentration  $c$  according to the relation

$$\phi = \bar{v}_h c \quad (6)$$

Viscosity measurements were performed on silica suspensions in the concentration range  $0 < c < 0.06 \text{ gm/cm}^3$  at  $25 \pm 0.1^\circ\text{C}$ . The measurements were carried out in a Brookfield viscometer at three different shearing rates. From these experiments we found that the viscosity of the suspensions was independent of the shearing rates and thus the suspensions behaved as Newtonian fluids. Very accurate viscosity data were next ob-

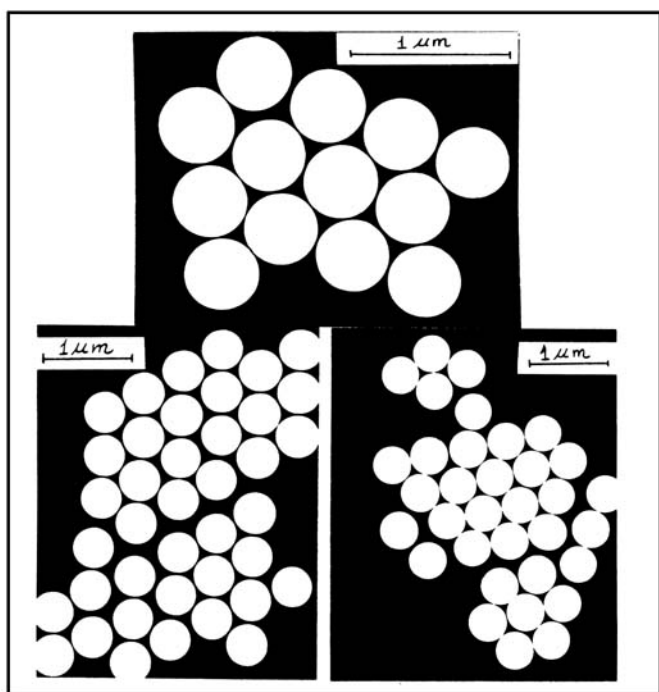


Figure 3a. Electron micrographs of coated silica particles of type  $S_1$ .

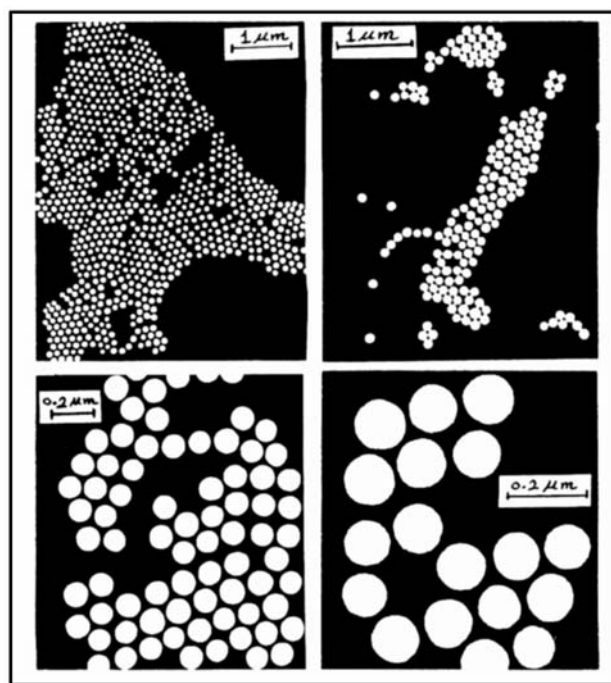


Figure 3c. Electron micrographs of coated silica particles of type  $S_3$ .

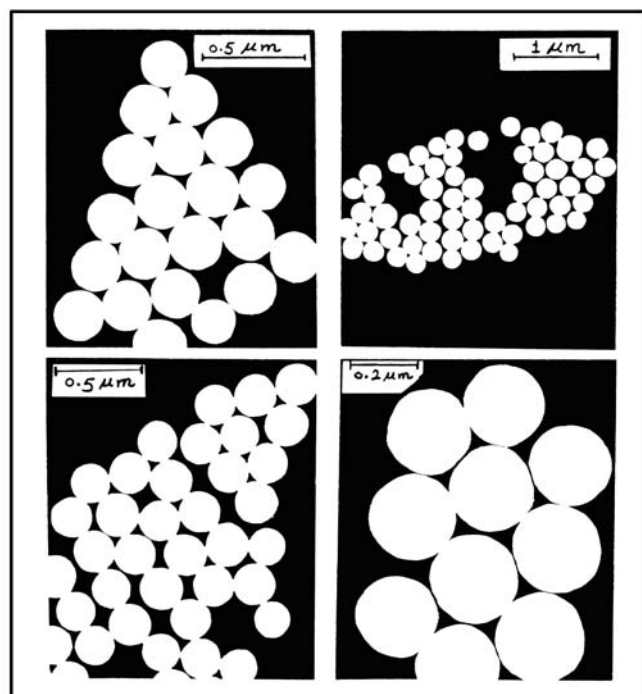


Figure 3b. Electron micrographs of coated silica particles of type  $S_2$ .

tained using Cannon-Fenske tubes immersed in a water bath at  $25 \pm 0.1^\circ\text{C}$ . The experimental data in the dilute concentration range were fitted to the Einstein relation

$$\frac{\eta}{\eta_0} = 1 + 2.5\phi \quad (7)$$

and the values of  $\bar{v}_h$  for the three particle species were accordingly determined. The results are listed in Table 3.

Sedimentation experiments were performed at  $25 \pm 0.1^\circ\text{C}$  in the concentration range between  $c = 0.0069$  and  $0.6903 \text{ gm/cm}^3$ . The experimental data extrapolated to zero concentration provided Stokes velocities for the particles. Measured values for the Stokes velocities and the hydrodynamic specific volumes were next used in Stokes law to determine the hydrodynamic radius  $a_h$  of the particles for the three particle species. The results are listed in Table 3. Comparison of the electron microscopy results for  $a_{EM}$  with the data obtained for  $a_h$  from the Stokes velocities for the particles (given in Table 3) shows that the former technique yields a smaller radius than the latter one. The decrease in size is a result of radiation damage that occurs during the electron microscopy measurements (van Hel-

Table 3. Characterization of Organophilic Silicas

	Particle Type		
	$S_1$	$S_2$	$S_3$
$a_{EM}$ (nm)	$242 \pm \sigma$	$130 \pm \sigma$	$65 \pm \sigma$
$\sigma$ (nm)	12	7	4.5
Percentage	5	5	7
Standard Dev. in Size			
$a_h$ (nm)	$252 \pm 5$	$138 \pm 4$	$74 \pm 2$
$\bar{v}_l$ ( $\text{cm}^3/\text{g}$ )	0.484	0.520	0.562
$\bar{v}_h$ ( $\text{cm}^3/\text{g}$ )	0.490	0.536	0.594
$U_o \times 10^5$ (cm/s)	$1.95 \pm 0.05$	$0.50 \pm 0.01$	$0.12 \pm 0.004$
Esterification Temperature ( $^\circ\text{C}$ )	300	205	200
Esterification Time (Hr)	10	8	5
% Carbon Content (W/W)	1.97	4.46	7.92

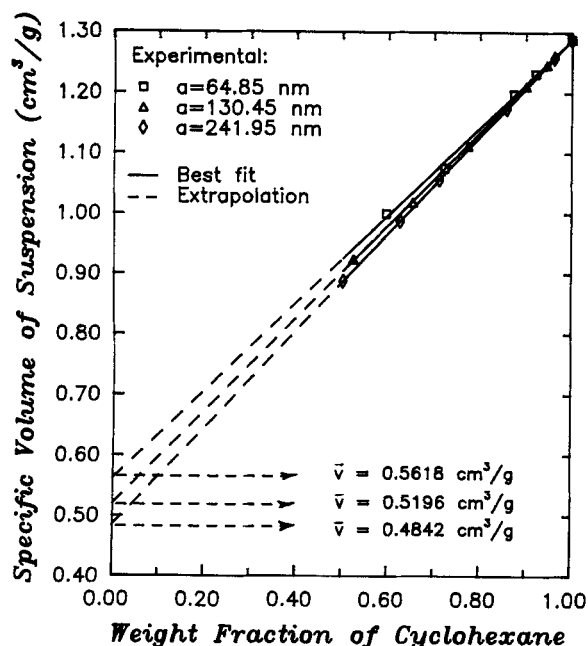


Figure 4. Specific volume of silica suspensions vs. weight fraction of cyclohexane.

den and Vrij, 1980). A slight difference in size is therefore expected, because the aliphatic chain molecules will be expanded in a good solvent, contrary to a more collapsed configuration in the dry phase.

### Hindered Settling Experiments

Monodisperse settling experiments were carried out for the  $S_1$ ,  $S_2$ , and  $S_3$  coated silica particles in cyclohexane. The volume fractions of the particles in the experiments were varied throughout the ranges  $0.0301 < \phi < 0.3039$ ,  $0.0048 < \phi < 0.37$ , and  $0.0041 < \phi < 0.3311$  for the  $S_1$ ,  $S_2$ , and  $S_3$  particles, respectively. All tests were carried out in vertical square vessels with borosilicate glass wall (1.5 mm thick) and having inside dimensions of 30 cm high and 1.6 cm by 1.6 cm in cross section. Each vessel was equipped with a special lid to prevent solvent evaporation and was mounted vertically on a specially constructed base made out of plexiglass. The suspensions were prepared outside the sedimentation vessels in 100 mL beakers. The quantity of suspension prepared in a batch was not more than 50 mL which was sufficient to fill a sedimentation vessel to about 5 cm from the top with little left over. For various particle concentrations, accurately known weights of particles and fluid were introduced into a beaker and the beaker with its contents covered firmly was sonicated for about half an hour. The suspension was next transferred to the sedimentation vessel and the vessel was carefully mounted in a vertical position in a thermostated air bath maintained at  $25 \pm 0.1^\circ\text{C}$ . After allowing the system to reach thermal equilibrium, the suspension was homogenized by making 20 sweeps with a glass stirrer. Care was taken to not entrain any air bubbles through the liquid-air interface. At the cessation of stirring, a clock was started to mark the beginning of sedimentation.

For concentrated suspensions ( $\phi > 0.05$ ), the solid-liquid interface at the top of the suspension was sufficiently sharp that its location could be measured to better than 0.01 mm using a cathatometer. The interface position was recorded at time

intervals of several hours over periods ranging from 100 to 1,000 hours depending on the concentration and the size of the particles. Typically, six measurements of the interface location as function of time were made for each suspension. After the interface had fallen over a substantial height (typically about 2 to 4 cm), the readings were stopped. A plot of interface height vs. position was then made and the slope of the best fit line obtained by regression analysis was taken to represent the sedimentation velocity of the suspension. For each suspension, the experiment was repeated at least four times and the mean value was used for the sedimentation velocity. Reproducibility was better than 3.5% of the mean values.

For dilute suspensions ( $\phi < 0.05$ ), the interface was less distinct than at high concentrations and its location could not be determined visually with absolute certainty. The observed spreading of the interface at the top of a sedimenting suspension is usually attributed to particle polydispersity as well as to the effect of particle diffusion. As a consequence of hindered settling, however, this spreading is reduced as the particle concentration is increased. For dilute suspensions, the fall speed of the particles in the diffuse interface was measured using the light extinction technique developed by Davis and co-workers (1988). This technique involves passing a thin horizontal slit of light through the suspension in order to measure the particle volume fraction at any location within the diffuse interface. A light beam from a 2 mW He-Ne laser (Uniphase Corporation) passes through a set of cylindrical glass lenses (Melles-Griot). These lenses expand the 0.62 mm diameter beam into a horizontal slit of parallel rays approximately 1 cm wide and 0.06 cm high. The flat beam passes through the sedimentation vessel and the light out of the vessel is converged through another lens and then focused onto the surface of a photodiode. The voltage signal from the photodiode, which is proportional to the transmitted light intensity, is then recorded through an analog-to-digital converter into a microcomputer. The laser, lenses, and photosensor were mounted on a horizontal support. This support is connected to a vertical screw shaft which is driven by a reversible stepper motor. The laser optics assembly can therefore be moved up and down the sedimentation vessel by means of the stepper motor. The whole system was contained inside a temperature-controlled air bath which was kept at  $25 \pm 0.1^\circ\text{C}$ . A typical example of the raw transmitted light intensity vs. distance along the interface is shown in Figure 5. The data in this figure were obtained by moving the optical system downward along the sedimentation vessel. As can be seen, above the interface, the intensity is a constant equal to that of the clear liquid,  $I_o$ . While below the interface the intensity is again constant and is equal to that of the bulk suspension,  $I_\infty$ . In general, it took less than one minute to scan the diffuse interface. As pointed out by Davis and co-workers (1988), the sedimentation velocity of the suspension may be taken equal to the rate of fall of the isoconcentration plane within the interface where  $\phi$  is equal to one-half of the particle volume fraction  $\phi_o$  in the bulk suspension. When  $\phi = \phi_o/2$ , the corresponding transmitted light,  $I_{1/2}$ , was determined from calibration curves of light intensity vs. particle concentration. The majority of these calibration curves closely approximated Beer's law. Under these conditions,  $I_{1/2}$  was taken equal to the geometric mean between the light intensity transmitted through the bulk suspension,  $I_\infty$ , and that for the clear liquid,  $I_o$ .

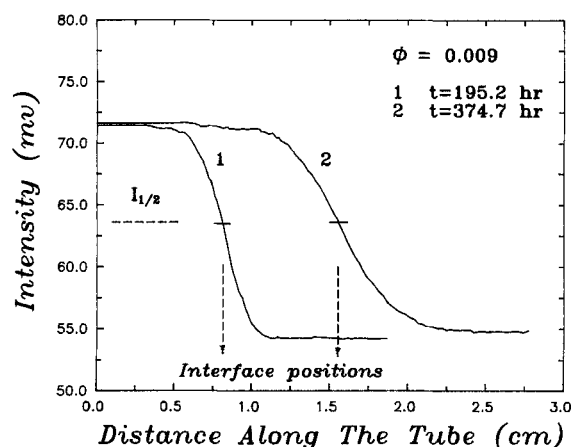


Figure 5. Light intensity data for a monodisperse suspension of the  $S_3$  particles with  $\phi = 0.009$ .

Bidisperse sedimentation experiments were also carried out using binary mixtures of  $S_1$  and  $S_2$  particles,  $S_2$  and  $S_3$  particles, and  $S_1$  and  $S_3$  particles in cyclohexane. Varying proportions of each size were used and the total particle volume fraction  $\phi_t$  ranged from 0.01 to 0.42. In these binary suspensions, the particles were distinct in size as well as density with the larger size particles also having a larger density. When such suspensions are subjected to sedimentation, the large particles have higher settling velocities than the small ones and therefore four zones are formed during the course of sedimentation (Davis and Acrivos, 1985). From the top downwards these consists of: (i) clear liquid, (ii) an upper sedimenting zone where only small particles are settling, (iii) a lower sedimenting zone where both particle species are present with concentrations equal to their initial concentrations in the initially uniform suspension, and (iv) a sediment layer. Let suffixes  $S$  and  $L$  apply to the small and large particles, respectively, and suffixes 1 and 2 apply to the upper and lower sedimenting zones. Accordingly, the settling velocities and concentrations in the lower zone may be denoted by  $U_{L,2}$ ,  $U_{S,2}$ ,  $\phi_{L,2}$  and  $\phi_{S,2}$ . The settling velocity and concentration of the small particles in the upper sedimenting zone are denoted by  $U_{S,1}$  and  $\phi_{S,1}$ . Evidently, the settling velocity of the large particles in the lower zone,  $U_{L,2}$ , corresponds to the rate of fall of the lower interface, while  $U_{S,1}$  corresponds to the rate fall of the upper interface. The interface velocities  $U_{L,2}$  and  $U_{S,1}$  were measured experimentally and the data were compared with predictions from available theoretical models.

For concentrated bidisperse suspensions ( $\phi_t > 0.15$ ), the range of concentrations for the two particle species was so chosen that both upper and lower interfaces of the sedimenting suspension were clearly discernible and their positions could be monitored visually using a cathatometer. For dilute suspensions ( $\phi_t < 0.07$ ), the light extinction method described earlier was used to measure the fall velocities of both interfaces. As the light assembly moved downwards along the sedimentation vessel, the transmitted light intensity decreased gradually from  $I_\infty$  (light intensity through the clear liquid) to  $I_1$  (light intensity through the upper sedimenting zone) and then again decreased gradually from  $I_1$  to  $I_2$  (the light intensity through the lower sedimenting zone). The gradual change in the transmitted light intensity indicated that the interfaces were not sharp in the dilute suspensions. The interfaces, however, became sharper

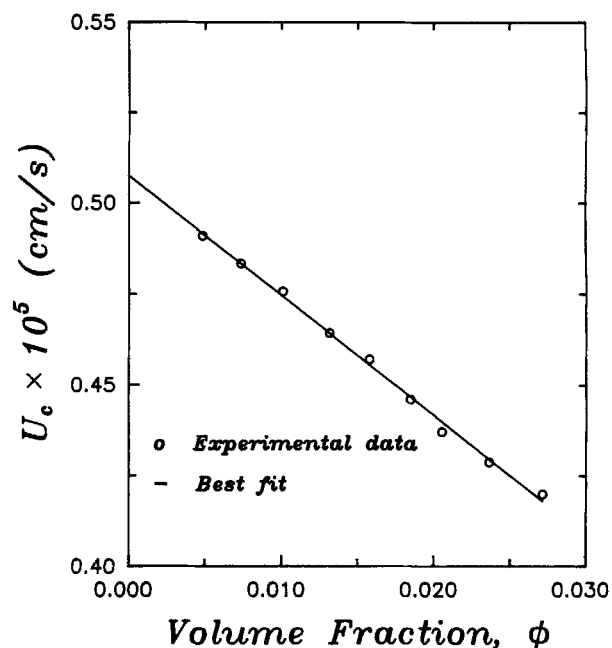


Figure 6. Hindered settling data for coated silica particles of type  $S_2$  in cyclohexane at dilute concentrations.

as the particle concentration increased. The light intensity data were used to obtain the interface velocities in a manner similar to that used for monodisperse suspensions.

## Results and Discussion

### Monodisperse suspensions

The hindered settling data for monodisperse suspensions are presented in Figures 6 through 10. For dilute suspensions, the settling data for the  $S_2$  and  $S_3$  particles over the concentration range  $0 < \phi < 0.03$  are shown in Figures 6 and 7. The solid lines in these figures represent the best fit linear regression of the form given by Eq. 3. As can be seen, the solid lines fit the data very well with regression coefficients larger than 0.98. The regression yielded the Stokes velocities listed in Table 3 and the  $O(\phi)$  coefficients listed in Table 1. The results for the  $O(\phi)$  coefficients of  $6.5 \pm 0.3$  and  $6.51 \pm 0.4$  for the  $S_2$  and  $S_3$  particles, respectively, are not statistically different from the theoretical prediction of 6.55 given by Batchelor (1972).

The monodisperse settling data for the  $S_1$ ,  $S_2$ , and  $S_3$  particles over the entire concentration range ( $0 < \phi < 0.37$ ) were correlated using the following Richardson-Zaki form:

$$U = U_o(1 - \phi)^n \quad (8)$$

The first-order expansion of this equation agrees exactly with Batchelor's equation for  $n = 6.55$ . Figure 8 is a Richardson-Zaki plot where  $\log U$  is plotted against  $\log(1 - \phi)$ . The solid lines in this plot represent the best fit of the experimental data using linear regression. Clearly, the Richardson-Zaki correlation provides an excellent fit of the data. The best fit values for the Stokes velocities for the  $S_2$  and  $S_3$  particles from the Richardson-Zaki plot agree within 3% with the Stokes velocities obtained from Figures 6 and 7. In addition, the best fit

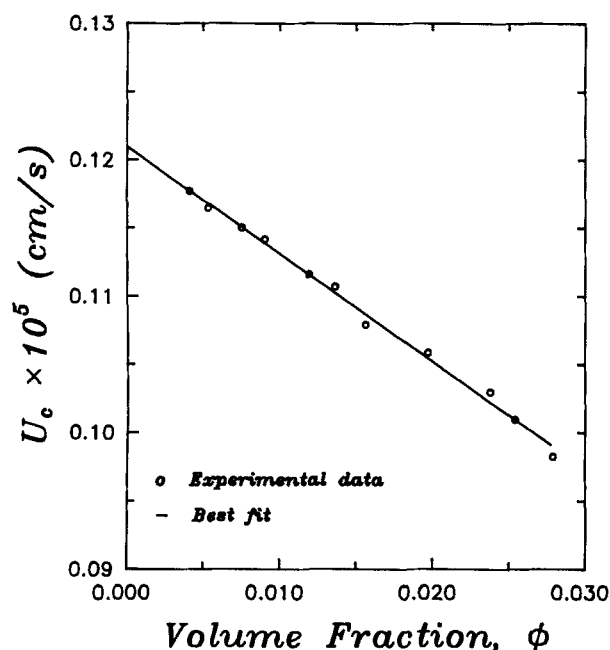


Figure 7. Hindered settling data for coated silica particles of type  $S_3$  in cyclohexane at dilute concentrations.

values for the exponent  $n$  from the Richardson-Zaki plot are  $6.21 \pm 0.3$ ,  $6.39 \pm 0.4$ , and  $6.41 \pm 0.2$  for the  $S_1$ ,  $S_2$ , and  $S_3$  particles, respectively. These values are not statistically different from the value 6.55. Thus, the monodisperse sedimentation data over a wide concentration range are well represented by the following correlation:

$$\frac{U}{U_o} = (1 - \phi)^{6.55} \quad (9)$$

It was also of interest to compare the results obtained in the

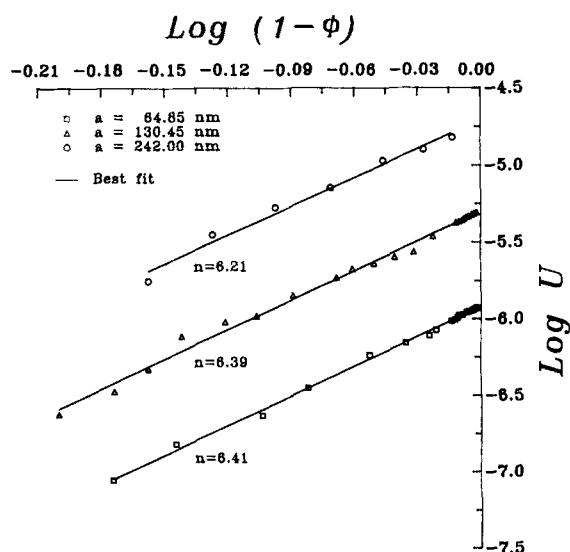


Figure 8. Hindered settling data for coated silica particles of type  $S_1$ ,  $S_2$ , and  $S_3$  in cyclohexane at high concentrations.

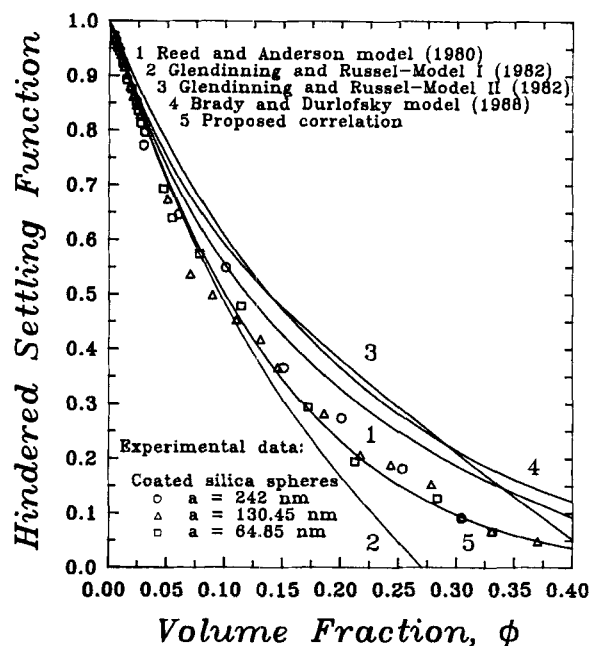
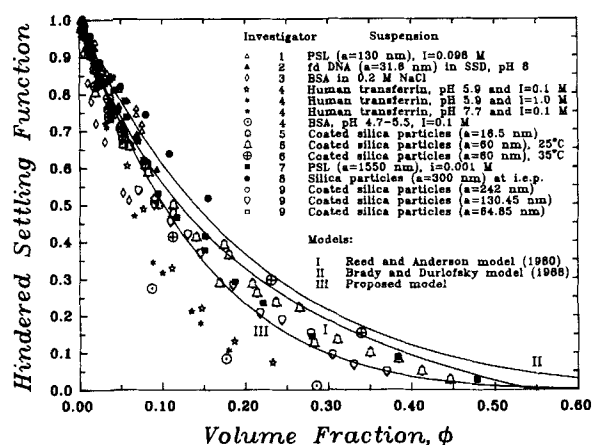


Figure 9. Comparison of experimental results for the hindered settling function with predictions from the proposed correlation.

present work with predictions from other models in the literature. This comparison is shown graphically in Figure 9. In this figure, the data are plotted as  $U/U_o$  vs.  $\phi$ , where  $U_o$  is the Stokes velocity obtained from the Richardson-Zaki plot. As can be seen from Figure 9, model II of Glendinning and Russel (Eq. 75 in their 1982 article) agrees with the data only in the very dilute concentration range. Their model I (Eq. 41 in their article), however, represents the data fairly well up to  $\phi \approx 0.15$ . For  $\phi > 0.15$ , the model underpredicts the data considerably and predicts negative values for  $U/U_o$  at concentrations larger than 0.27. The models by Reed and Anderson (1980) and Brady and Durlofsky (1988) predict the observed trend in  $U/U_o$  with increasing  $\phi$  over the entire concentration range. The predictions, however, are higher than the experimental data at high concentrations. The average deviations of predicted values of  $U/U_o$  from the experimental points are about 23% for the Reed-Anderson model and 30% for the Brady-Durlofsky model. The proposed correlation (Eq. 9) on the other hand represents the data fairly well over the entire concentration range. The correlation predicts the data with a maximum deviation of 15% and can be applied for all particle volume fractions from  $\phi = 0$  to  $\phi \approx 0.4$ . The absolute average percent deviation of all the experimental points from Eq. 9 is 4.51%.

Sedimentation data from other investigations are summarized in Table 1 and also plotted in Figure 10. As alluded to earlier in the introduction, only the DNA data of Newman et al. (1974) and the data of Kops-Werkhoven and Fijnaut (1981, 1982) deserve comparison with available models. The measured values for the  $O(\phi)$  coefficient of  $6.7 \pm 0.8$  from the Newman et al. data and  $6.0 \pm 1$  from the Kops-Werkhoven and Fijnaut data are in satisfactory agreement with the theoretical value of 6.55 due to Batchelor. Notice, however, that values for the  $O(\phi)$  coefficient obtained from our particles compare more





**Figure 10.** Comparison of published experimental data for sedimentation of monodisperse colloidal suspensions with predictions from the Reed-Anderson model, the Brady-Durlofsky model and the proposed correlation.

Investigators: (1) Cheng and Schachman (1955), (2) Newman et al. (1974), (3) Kitchen et al. (1976), (4) Lundh (1980), (5) Kops-Werkhoven and Fijnaut (1981), (6) Kops-Werkhoven and Fijnaut (1982), (7) Buscall et al., (1982), (8) Tackie et al. (1983), and (9) Proposed Correlation.

favorably with Batchelor's value than the values reported by Newman et al. and Kops-Werkhoven and Fijnaut.

The data by Kops-Werkhoven and Fijnaut (1982) covered a wide concentration range ( $0 < \phi < 0.44$ ) and may thus be compared with predictions from the models. These comparisons give average deviations of 14.15% for the Reed-Anderson model, 23% for the Brady-Durlofsky model, and 14.81% for the proposed correlation. Combining our data with the data

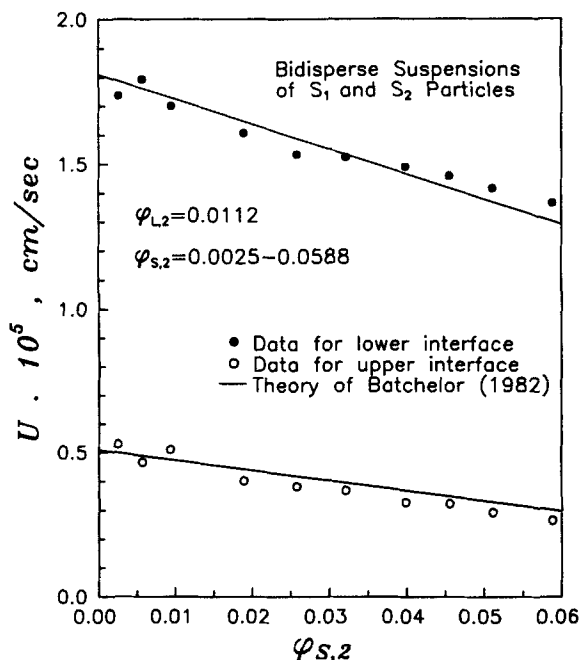


**Figure 11.** Hindered settling data for a bidisperse suspension of the  $S_1$  and  $S_2$  particles with  $\phi_{L,2} = 0.0112$ .

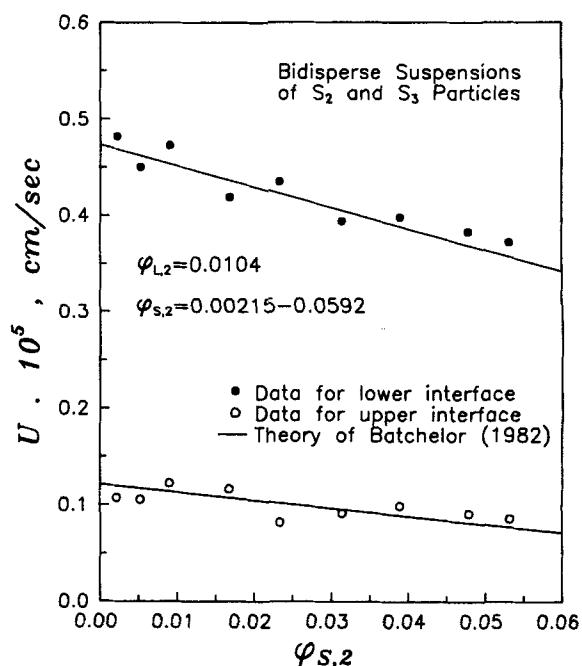


**Figure 12.** Hindered settling data for a bidisperse suspension of the  $S_2$  and  $S_3$  particles with  $\phi_{L,2} = 0.0104$ .

by Newman et al. and Kops-Werkhoven and Fijnaut, we obtain values of 16.85, 17.96, and 8.82% for the average deviations with the Reed-Anderson model, the Brady-Durlofsky model and the present correlation, respectively. We may therefore conclude that the proposed correlation gives satisfactory predictions for the settling rate of colloidal suspensions of uncharged rigid spheres over a wide range of concentration. We should remark that our study has been confined to sedimentation of suspensions with particle volume fraction less than 0.4. Sedimentation data at higher volume fractions in the vicinity of the disorder-order transition have been recently reported by Paulin and Ackerson (1990).

### Bidisperse suspensions

The hindered settling data for dilute bidisperse suspensions are presented in Figures 11 through 16. In Figures 11, 12, and 13 the volume fraction of the large particles,  $\phi_L$ , was held fixed while the volume fraction of the small particles,  $\phi_S$ , was allowed to vary in the suspension. In Figures 14, 15, and 16, however,  $\phi_S$  was held fixed and  $\phi_L$  was allowed to vary. The solid lines in these figures represent the theory of Batchelor (1982) for the lower and upper interface velocities,  $U_{L,2}$  and  $U_{S,1}$ . Batchelor's theory is based on pairwise particle interactions and is thus limited to dilute suspensions. According to this theory, the hindered settling velocity  $U_i$  of a particle of species  $i$  in a polydisperse suspension of  $N$  discrete particles is given by

$$U_i = U_{o,i} \left( 1 + \sum_{j=1}^N S_{ij} \phi_j \right) \quad (10)$$

where  $U_{o,i}$  is the Stokes velocity of species  $i$ ,  $\phi_j$  is the volume fraction of species  $j$  in the mixture,  $S_{ij}$  are dimensionless sedi-

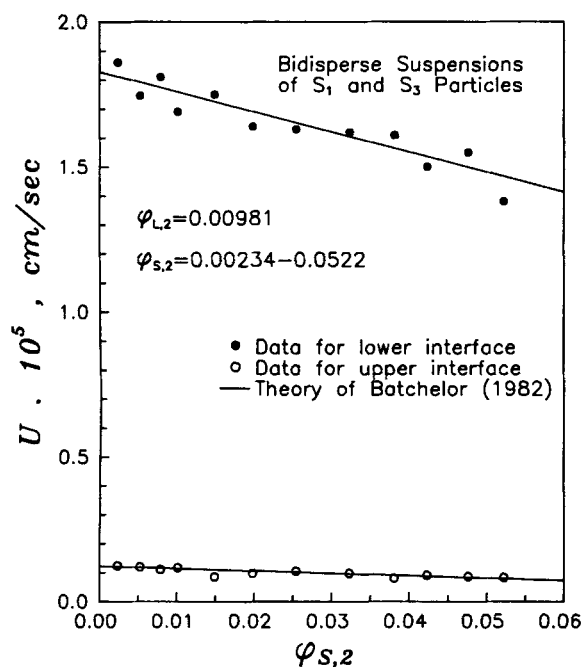


Figure 13. Hindered settling data for a bidisperse suspension of the  $S_1$  and  $S_3$  particles with  $\phi_{L,2} = 0.00981$ .

mentation coefficients that depend on the radius ratio,  $\lambda = a_j/a_i$ , and the relative density ratio,  $\gamma = (\rho_j - \rho_f)/(\rho_i - \rho_f)$ , plus any Brownian or interparticle forces that may be present. Values of the sedimentation coefficients were calculated by Batchelor and Wen (1982) for a wide variety of conditions of the

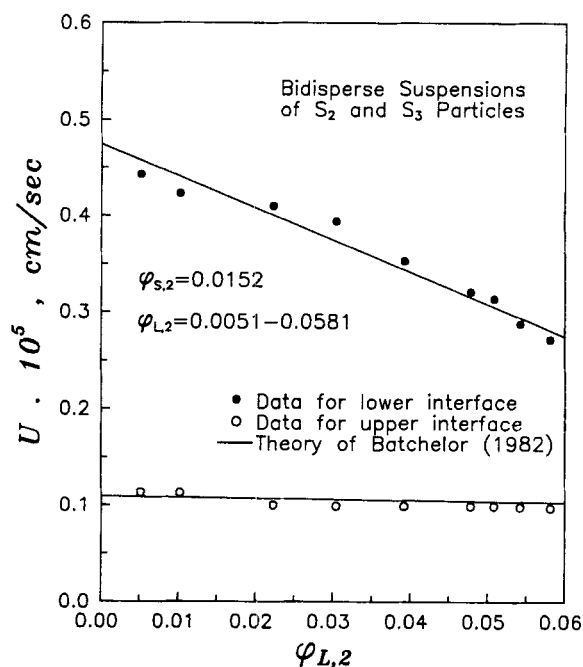


Figure 15. Hindered settling data for a bidisperse suspension of the  $S_2$  and  $S_3$  particles with  $\phi_{S,2} = 0.0152$ .

two interacting species. At small Peclet number and in the absence of interparticle forces, values of the  $S_{ij}$ 's were taken from Table 3 of Batchelor and Wen and used to calculate the settling velocities for bidisperse suspensions of the  $S_1$ ,  $S_2$ , and  $S_3$  particles in cyclohexane. The results of these calculations yield the following expressions:

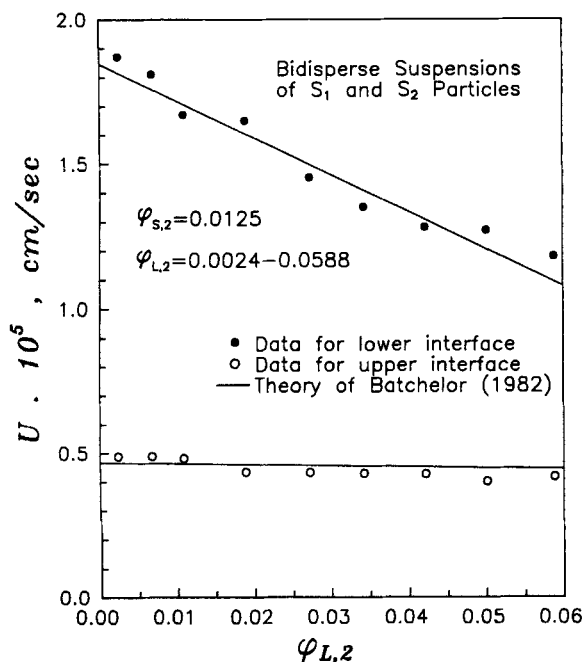


Figure 14. Hindered settling data for a bidisperse suspension of the  $S_1$  and  $S_2$  particles with  $\phi_{S,2} = 0.0125$ .

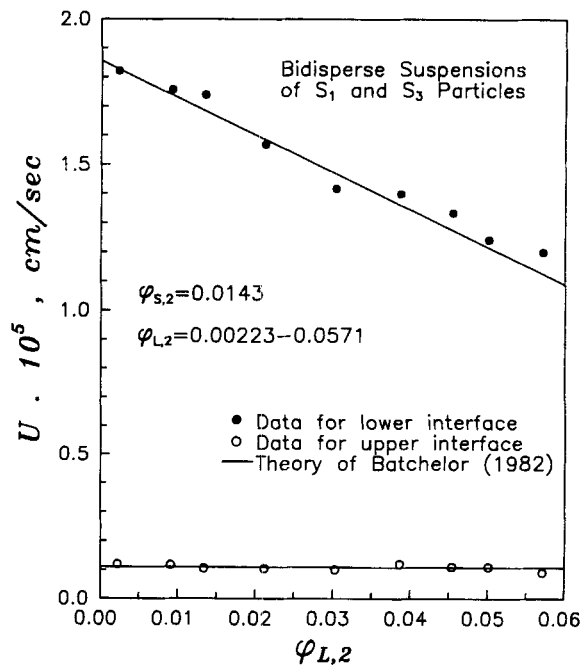


Figure 16. Hindered settling data for a bidisperse suspension of the  $S_1$  and  $S_3$  particles with  $\phi_{S,2} = 0.0143$ .

$$U_L = U_{o,L}(1 - 6.55\phi_L - 4.43\phi_S) \quad (11a)$$

$$U_S = U_{o,S}(1 - 12.52\phi_L - 6.55\phi_S) \quad (11b)$$

for a bidisperse suspension of the  $S_1$  and  $S_2$  particles.

$$U_L = U_{o,L}(1 - 6.55\phi_L - 4.31\phi_S) \quad (12a)$$

$$U_S = U_{o,S}(1 - 13.26\phi_L - 6.55\phi_S) \quad (12b)$$

for a bidisperse suspension of the  $S_2$  and  $S_3$  particles.

$$U_L = U_{o,L}(1 - 6.55\phi_L - 3.54\phi_S) \quad (13a)$$

$$U_S = U_{o,S}(1 - 32.57\phi_L - 6.55\phi_S) \quad (13b)$$

for a bidisperse suspension of the  $S_1$  and  $S_3$  particles.

In a typical experiment, one starts with a uniform suspension of known concentrations for the large and small particles. According to our notation, these initial concentrations are denoted by  $\phi_{L,2}$  and  $\phi_{S,2}$ , respectively. The observed rate of fall of the lower interface corresponds to  $U_{L,2}$ . Theoretical predictions for  $U_{L,2}$  are readily calculated from Eqs. 11a, 12a, or 13a with  $\phi_L$  and  $\phi_S$  replaced by  $\phi_{L,2}$  and  $\phi_{S,2}$ , respectively. Note that the volume fractions of both particle species in the lower zone of the sedimenting suspension are equal to their initial values.

For the upper zone, the volume fraction of the slower-settling species,  $\phi_{S,1}$ , is determined from

$$\phi_{S,1} = \frac{U_{L,2} - U_{S,2}}{U_{L,2} - U_{S,1}} \phi_{S,2} \quad (14)$$

This expression may be derived through a particle flux continuity requirement for the slower-settling species crossing the lower interface (Smith, 1966). Incidentally, the slower-settling species corresponds to the smaller size particles in the present suspensions. Moreover, since the upper zone contains only the slower-settling particles, Eq. 3 can be readily applied to give  $U_{S,1}$  as

$$U_{S,1} = U_{o,S}(1 - 6.55\phi_{S,1}) \quad (15)$$

Equations 14 and 15 may be solved simultaneously for  $\phi_{S,1}$  and  $U_{S,1}$ . Evidently,  $U_{S,1}$  corresponds to the rate of fall of the upper interface.

As can be seen from Figures 11 through 16, the agreement between the experimental data and Batchelor's theory is fairly good. The average percent deviation of predicted values from measured values is about 7 percent. This deviation is comparable with the reproducibility of the experimental results. We should point out that in constructing the solid lines (Batchelor's predictions) in Figures 11 through 16, the Stokes velocities used are from the linear regression of the monodisperse results reported earlier.

For concentrated bidisperse suspensions ( $\phi_i > 0.15$ ), representative plots are shown in Figures 17 and 18 for binary suspensions of the  $S_1$  and  $S_2$  particles. Plots for the other particle mixtures are essentially similar. Although a rigorous theory for sedimentation in concentrated polydisperse suspen-

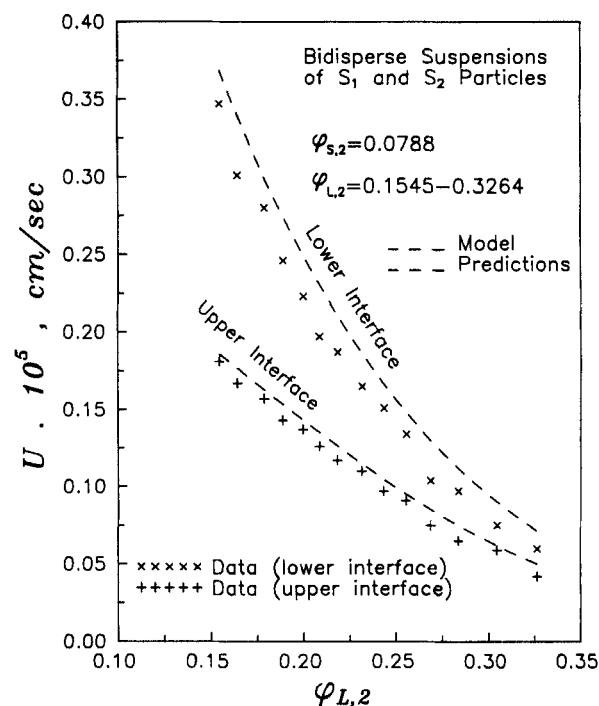


Figure 17. Hindered settling data for a bidisperse suspension of the  $S_1$  and  $S_2$  particles with  $\phi_{S,2} = 0.0788$ .

sions appears to be lacking at the present time, a satisfactory interpretation of the experimental results could be made based on Eq. 9. This equation can be applied to calculate approximately the sedimentation rate of a particular particle species

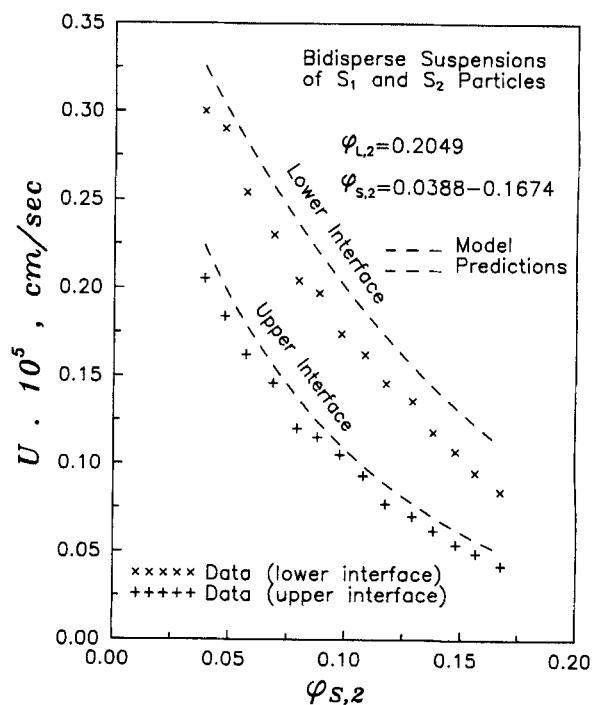


Figure 18. Hindered settling data for a bidisperse suspension of the  $S_1$  and  $S_2$  particles with  $\phi_{L,2} = 0.2049$ .

in a polydisperse suspension provided that the hindered settling function involves the total local concentration of all particle species in the mixture. With this notion in mind, consider a suspension of a mixture of large and small particles with volumetric concentrations  $\phi_L$  and  $\phi_S$ , respectively. For each of the spheres therefore settling on its own, Eq. 9 gives

$$\frac{U_L}{U_{o,L}} = (1 - \phi_L)^{6.55} = e^{6.55} \quad (16)$$

and

$$\frac{U_S}{U_{o,S}} = (1 - \phi_S)^{6.55} = e^{6.55} \quad (17)$$

where  $e$  is the voidage of the suspension. Then considering the velocities of the particles relative to the fluid,  $U_L/e$  and  $U_S/e$ , respectively:

$$U_L/e = U_{o,L} e^{5.55} \quad (18)$$

and

$$U_S/e = U_{o,S} e^{5.55} \quad (19)$$

When the particles of two sizes are settling together, the upflow of displaced fluid is caused by the combined effects of the sedimentation of the large and small particles. Denoting this upward velocity by  $U_F$ , the sedimentation rates  $U_L$  and  $U_S$  may be obtained by deducing  $U_F$  from the velocities relative to the fluid. Thus:

$$U_L = U_{o,L} e^{5.55} - U_F \quad (20)$$

and

$$U_S = U_{o,S} e^{5.55} - U_F \quad (21)$$

Then, since the volumetric flow of displaced fluid upwards is equal to the total volumetric flow rate of particles downwards, it follows that

$$U_F e = (U_{o,L} e^{5.55} - U_F) \phi_L + (U_{o,S} e^{5.55} - U_F) \phi_S \quad (22)$$

or

$$U_F = e^{5.55} (U_{o,L} \phi_L + U_{o,S} \phi_S) \quad (23)$$

since  $e + \phi_L + \phi_S = 1$ . Then substituting from Eq. 23 into Eqs. 20 and 21, we obtain the following expressions for the sedimentation velocities in the lower zone of a sedimenting suspension:

$$U_{L,2} = (1 - \phi_{L,2} - \phi_{S,2})^{5.55} [U_{o,L} (1 - \phi_{L,2}) - U_{o,S} \phi_{S,2}] \quad (24)$$

$$U_{S,2} = (1 - \phi_{L,2} - \phi_{S,2})^{5.55} [U_{o,S} (1 - \phi_{S,2}) - U_{o,L} \phi_{L,2}] \quad (25)$$

For the upper zone, Eq. 14 still holds for the volume fraction  $\phi_{S,1}$  while Eq. 15 is replaced by

$$U_{S,1} = U_{o,S} (1 - \phi_{S,1})^{6.55} \quad (26)$$

Equations 24 and 26 for the velocities of the lower and upper interfaces are represented by the dashed curves in Figures 17 and 18. As can be seen, all the data fall below the dashed curves. The predicted velocities for both interfaces are over-predicted in both figures by between 5 and 25%. Because for a given system the experimental and predicted results show an almost constant difference, the percentage difference is greatest at high concentrations when the effects of particle interactions are greatest. It should be pointed out that the application of Eq. 9 to a polydisperse system implies that the model treats interactions between unlike particles in the same way as it does those between like particles. This in turn implies that inter-particle interactions, which must become increasingly important both as the total concentration increases and as the relative velocity of the particles increases, are not completely accounted for. Accordingly, Eqs. 24 through 26 can only serve as upper bounds for the sedimentation velocities. This is well demonstrated by the present results.

## Acknowledgment

The authors wish to thank Dr. William B. Russel for helpful discussions during the execution of this work. The authors also wish to thank Dr. R. H. Davis for providing details regarding the light extinction equipment.

## Notation

- $a$  = particle radius
- $a_{EM}$  = particle radius from electron microscopy
- $a_h$  = hydrodynamic particle radius
- $c$  = particle mass concentration
- $D_o$  = Brownian diffusion coefficient at infinite dilution
- $e$  = voidage of suspension
- $f(\phi)$  = hindered settling function
- $g$  = gravitational acceleration constant
- $k_B$  = Boltzmann constant
- $n$  = exponent in Richardson-Zaki correlation
- $Pe$  = Peclet number
- $S_{ij}$  = sedimentation coefficient
- $T$  = absolute temperature
- $U$  = hindered settling velocity
- $U_F$  = upward velocity of displaced fluid
- $U_o$  = Stokes settling velocity of an isolated sphere
- $\bar{v}_h$  = hydrodynamic specific volume
- $\bar{v}_i$  = partial specific volume

## Greek letters

- $\gamma$  = relative density ratio,  $(\rho_j - \rho_f)/(\rho_i - \rho_f)$
- $\Delta\rho$  = density difference,  $(\rho_s - \rho_f)$
- $\eta$  = viscosity of suspension
- $\eta_o$  = viscosity of suspending medium
- $\lambda$  = radius ratio,  $a_j/a_i$
- $\rho$  = density
- $\rho_f$  = fluid density
- $\rho_s$  = solid density
- $\phi$  = particle volume fraction

## Subscripts

- 1 = for zone 1 (upper zone)
- 2 = for zone 2 (lower zone)
- $L$  = for the large particles
- $S$  = for the small particles

## Literature Cited

- Al-Naafa, M. A., "Sedimentation and Brownian Diffusion of Uncharged Rigid Spheres," PhD Thesis, Colorado School of Mines (1990).
- Ballard, C. C., E. C. Broge, R. K. Iler, D. S. John, and J. R. McWhorter, "Esterification of the Surface of Amorphous Silica," *J. Phys. Chem.*, **65**, 20 (1961).
- Batchelor, G. K., "Sedimentation in a Dilute Dispersion of Spheres," *J. Fluid Mech.*, **52**(2), 245 (1972).
- Batchelor, G. K., "Sedimentation in a Dilute Polydisperse System of Interacting Spheres. Part I. General Theory," *J. Fluid Mech.*, **119**, 379 (1982).
- Batchelor, G. K., and C. S. Wen, "Sedimentation in a Dilute Polydisperse System of Interacting Spheres. Part II. Numerical Results," *J. Fluid Mech.*, **124**, 495 (1982).
- Brady, J. F., and L. J. Durlofsky, "The Sedimentation Rate of Disordered Suspensions," *Phys. Fluids*, **31**, 717 (1988).
- Buscall, R., J. W. Goodwin, R. H. Ottewill, and Th. F. Tadros, "The Settling of Particles Through Newtonian and Non-Newtonian Media," *J. Colloid Interface Sci.*, **85**, 78 (1982).
- Cheng, P. Y., and H. K. Schachman, "Studies on the Validity of the Einstein Viscosity Law and Stokes' Law of Sedimentation," *J. Polym. Sci.*, **16**, 19 (1955).
- Davis, R. H., and A. Acrivos, "Sedimentation of Noncolloidal Particles at Low Reynolds Numbers," *Ann. Rev. Fluid Mech.*, **17**, 91 (1985).
- Davis, R. H., and K. H. Birdsell, "Hindered Settling of Semidilute Monodisperse and Polydisperse Suspensions," *AIChE J.*, **34**, 123 (1988).
- Davis, R. H., and M. A. Hassen, "Spreading of the Interface at the Top of a Slightly Polydisperse Sedimenting Suspension," *J. Fluid Mech.*, **196**, 107 (1988).
- Glendinning, A. B., and W. B. Russel, "A Pairwise Additive Description of Sedimentation and Diffusion in Concentrated Suspensions of Hard Spheres," *J. Colloid Interface Sci.*, **89**(1), 124 (1982).
- Hunter, R. J., *Foundations of Colloid Science*, Oxford University Press, New York (1987).
- Iler, R. K., "Silica Hydrosol Powder," U.S. Patent 2,801,185 (1957).
- Kitchen, R. G., B. N. Preston, and J. D. Wells, "Diffusion and Sedimentation of Serum Albumin in Concentrated Solutions," *J. Polymer Sci.: Symp. No. 55*, pp. 39-49 (1976).
- Kops-Werkhoven, M. M., and H. M. Fijnaut, "Dynamic Light Scattering and Sedimentation Experiments on Silica Dispersions at Finite Concentrations," *J. Chem. Phys.*, **74**, 1618 (1981).
- Kops-Werkhoven, M. M., and H. M. Fijnaut, "Dynamic Behavior of Silica Dispersions Studied Near the Optical Matching Point," *J. Chem. Phys.*, **77**, 2242 (1982).
- Lundh, S., "Concentrated Protein Solutions in the Analytical Ultracentrifuge," *J. Polym. Sci.—Polym. Phys. Edition*, **18**, 1963 (1980).
- Mewis, J., W. J. Frith, T. A. Strivens, and W. B. Russel, "The Rheology of Suspensions Containing Polymerically Stabilized Particles," *AIChE J.*, **35**, 415 (1989).
- Newman, J., H. L. Swinney, S. A. Berkowitz, and L. A. Day, "Hydrodynamic Properties and Molecular Weight of fd Bacteriophage DNA," *Biochemistry*, **13**(23), 4832 (1974).
- O'Brien, R. W., "A Method for the Calculation of the Effective Transport Properties of Suspensions of Interacting Spheres," *J. Fluid Mech.*, **91**(1), 17 (1979).
- Paulin, S. E., and B. J. Ackerson, "Observation of a Phase Transition in the Sedimentation Velocity of Hard Spheres," *Phys. Rev. Lett.*, **64**, 2663 (1990).
- Prigogine, I., and R. Defay, *Chemical Thermodynamics*, John Wiley & Sons, New York (1954).
- Reed, C. C., and J. L. Anderson, "Hindered Settling of a Suspension at Low Reynolds Number," *AIChE J.*, **26**, 816 (1980).
- Smith, T. N., "The Sedimentation of Particles Having a Dispersion of Sizes," *Trans. Inst. Chem. Eng.*, **44**, T153 (1966).
- Stöber, W., A. Fink, and E. Bohn, "Controlled Growth of Monodisperse Silica Spheres in the Micron Size Range," *J. Colloid Interface Sci.*, **26**, 62 (1968).
- Tackie, E., B. D. Bowen, and N. Epstein, "Hindered Settling of Uncharged and Charged Submicrometer Spheres," *Ann. NY Acad. Sci.*, **404**, 366 (1983).
- van Helden, A. K., and A. Vrij, "Contrast Variation in Light Scattering: Silica Spheres Dispersed in Apolar Solvent Mixtures," *J. Colloid Interface Sci.*, **76**(2), 418 (1980a).
- van Helden, A. K., and A. Vrij, "Static Light Scattering of Concentrated Silica Dispersions in Apolar Solvents," *J. Colloid Interface Sci.*, **78**(2), 312 (1980b).
- van Helden, A. K., J. W. Jansen, and A. Vrij, "Preparation and Characterization of Spherical Monodisperse Silica Dispersions in Nonaqueous Solvents," *J. Colloid Interface Sci.*, **18**(2), 354 (1981).

Manuscript received July 25, 1991, and revision received May 21, 1992.